How to decide between competing efficiency droop models for GaN-based light-emitting diodes

Joachim Piprek[a)]
NUSOD Institute LLC, Newark, Delaware 19714-7204, USA

(Received 11 June 2015; accepted 10 July 2015; published online 20 July 2015)

GaN-based light-emitting diodes (LEDs) exhibit a strong efficiency droop with higher current injection, which has been mainly attributed to Auger recombination and electron leakage, respectively. Thus far, the few reports on *direct* measurements of these two processes do not confirm their dominating influence on the droop unambiguously. Advanced numerical simulations of experimental characteristics are shown to validate one or the other explanation by variation of uncertain material parameters. We finally demonstrate how the comparative simulation of temperature effects enables a clear distinction between both models. Contrary to common assumptions, the consistently measured efficiency reduction of blue LEDs with higher ambient temperature eliminates electron leakage as *primary* cause of the efficiency droop in these devices. © *2015 AIP Publishing LLC*.
[http://dx.doi.org/10.1063/1.4927202]

GaN-based light-emitting diodes (LEDs) are of major interest for applications in lighting, displays, sensing, biotechnology, medical instrumentation, and other areas, but their performance is handicapped by a significant efficiency reduction with increasing injection current (efficiency droop).[1,2] Different microscopic mechanisms have been proposed to explain the high-current efficiency droop, most prominently electron leakage from the quantum wells (QWs)[3] and Auger recombination inside the QWs,[4] respectively. Defect-related QW Shockley-Read-Hall (SRH) recombination limits the efficiency of industry-grade LEDs only at low current.[5] Very few direct measurements of either high-current mechanism have been published thus far, none of which establishes a dominating magnitude. All quantitative assessments of the efficiency droop are based on modelling and simulation. Different and partially contradicting models were shown to produce good agreement with measured efficiency vs. current characteristics. Thus, the search for the origin of the efficiency droop turned into a validation problem for GaN-LED efficiency models. Simple models that consider only one of the high-current droop mechanisms are unable to distinguish between competing explanations. Advanced numerical models that include all droop mechanisms still depend on various material parameters which are not exactly known. This parameter uncertainty often leaves enough room to let either mechanism dominate. Published droop simulations use not only different numerical codes and different parameter sets but also are applied to different device examples, thereby making a droop model comparison and validation even more difficult.

We here compare the two leading droop explanations by simulating the same measurements on the same device using an advanced numerical code (APSYS)[6] with two different sets of material parameters favouring one or the other mechanism. The self-consistent simulation solves the semiconductor carrier transport equations coupled with a quantum-mechanical model for the photon emission from the strained InGaN quantum wells. The built-in polarization charge at hetero-interfaces is calculated using a non-linear model.[7] Schrödinger and Poisson equations are solved iteratively for each quantum well in order to account for the quantum confined Stark effect. The carrier transport model includes drift and diffusion of electrons and holes, Fermi statistics, and thermionic emission at hetero-interfaces, which allows for electron leakage into the p-doped layers. Nonradiative recombination via the SRH mechanism is considered as well as Auger recombination inside the QWs. Incomplete ionization of Mg acceptors is also included, and the AlGaN acceptor energy is linearly scaled from 170 meV in p-GaN to 470 meV in p-AlN. Self-heating is not accounted for because all measurements are performed in pulsed operation. Further model details can be found elsewhere.[8]

In this comparative simulation exercise, the magnitudes of Auger recombination and electron leakage are varied by changing only two key material parameters: the Auger recombination coefficient C and the acceptor density N_A inside the AlGaN electron blocking layer (EBL). The EBL's ability to stop electron leakage strongly depends on N_A because negatively charged acceptors are able to compensate for positive polarization charges at the EBL interface to the multi-quantum well (MQW) active region.[9] However, not all of the Mg atoms become AlGaN acceptors,[10] so that this essential simulation parameter is typically smaller than expected, and the leakage current potentially much larger. While the Mg profile can be measured, the actual acceptor profile remains unknown. Electron leakage also depends on other material properties such as the EBL band offset and the polarization screening. We here employ a band offset of 50% and a screening factor of 0.5;[3] however, different sets of parameters may result in the same leakage current.[11] For simplicity, we keep these two parameters constant in all simulations and exclude field ionization effects, which depend on the unknown acceptor profile inside the EBL.[12]

The second crucial parameter, C, is even more uncertain. Auger recombination coefficients extracted from measurements strongly depend on the model used for extraction,

a)piprek@nusod.org

 © 2015 AIP Publishing LLC

This article is copyrighted as indicated in the article. Reuse of AIP content is subject to the terms at: http://scitation.aip.org/termsconditions. Downloaded to IP: 173.75.255.93 On: Mon, 20 Jul 2015 13:56:11

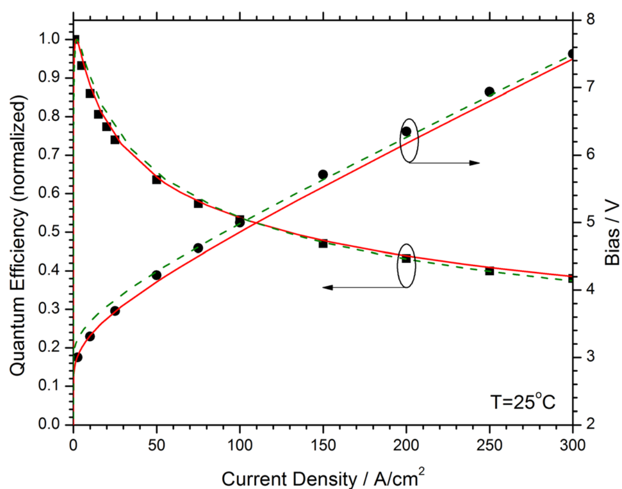

FIG. 1. Normalized quantum efficiency and bias vs. current density at room temperature (symbols—measurement, solid lines—simulation favouring Auger recombination, and dashed lines—simulation favouring electron leakage).

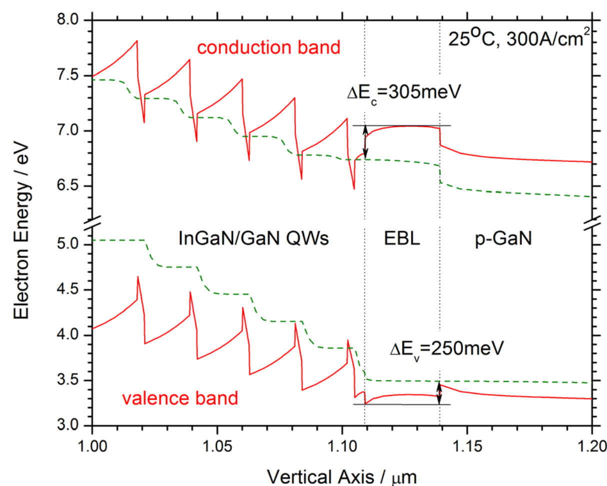

FIG. 2. Energy band diagram near the active region for a high acceptor density of $N_A = 10^{19}\,cm^{-3}$ inside the EBL (solid lines—band edges and dashed lines—quasi Fermi levels).

and reported InGaN values vary over two orders of magnitude.[13] Microscopic theories of *direct* Auger recombination in III-V semiconductors typically predict negligibly low C-coefficients for wide-gap materials such as GaN. Exceptions arise for bulk InGaN when higher conduction bands are included which lead to relevant direct Auger recombination near the resonance energy.[14–16] However, those models are unable to explain why the efficiency droop occurs over a wide wavelength range. Other publications suggest higher C-coefficients for *indirect* Auger transitions in bulk InGaN, involving phonons and alloy scattering,[17] but modeling details are still disputed.[18] Calculations for InGaN quantum wells are more complicated and very few results are published thus far. Initial computations for InGaN QWs give *direct* Auger coefficients on the order of $10^{-34}cm^6/s$.[19] More recent reports based on advanced band structure models indicate a strong influence of the well width,[20] and a surprising C-parameter enhancement with rising built-in polarization field.[21] Other authors predict similar field effects on InGaN QW Auger recombination,[22] as well as C-parameter reductions with graded QW interfaces,[23] but based on the cubic crystal structure which is not appropriate for practical wurtzite devices. Microscopic computations of *indirect* Auger recombination in InGaN quantum wells have not been published yet. Thus, we here utilize the Auger coefficient C as a second fit parameter.

As a practical example for our study, we employ published measurements on InGaN/GaN LEDs with peak emission near 440 nm.[24] The reference device comprises five 3-nm-thick InGaN/GaN quantum wells that are covered by a p-$Al_{0.13}Ga_{0.87}N$ EBL and a p-GaN cladding layer. Reported LED characteristics are depicted by symbols in Fig. 1. The current-voltage characteristic exhibits a turn-on bias near 3 V and a series resistance of 115 Ω. The peak quantum efficiency is measured below 5 A/cm^2 injection current density and drops by 62% as the current density is raised to 300 A/cm^2. This efficiency droop is now simulated in two different ways.

The first simulation assumes that the majority of Mg atoms form AlGaN acceptors ($N_A = 10^{19}\,cm^{-3}$). Figure 2 shows the energy band diagram for this case and illustrates the strong QW deformation due to the built-in polarization. EBL band bending caused by ionized acceptors contributes to a high electron barrier of 305 meV, which almost completely stops electron leakage. Without leakage, the measured efficiency characteristic is fitted by using a large QW Auger coefficient of $C = 5 \times 10^{-30}\ cm^6/s$ together with a SRH lifetime of 40 ns. Thus, the efficiency droop is dominantly caused by Auger recombination. The simulated efficiency and bias characteristics are both in good agreement with the measurements, the turn-on bias near 3 V is perfectly reproduced in this case (solid red lines in Fig. 1).

In the second simulation, the AlGaN acceptor density is reduced to $N_A = 2.6 \times 10^{18}\,cm^{-3}$, which lowers the EBL band bending and the EBL electron barrier to 195 meV and causes strong electron leakage. The EBL hole barrier rises from 250 meV to 288 meV. By suppressing QW Auger recombination ($C = 10^{-34}\ cm^6/s$), the measured characteristics are also reproduced quite well (dashed green lines in Fig. 1). At 300A/cm^2 total current density, 227 A/cm^2 are now consumed by electrons leaking into the p-doped layers. Correspondingly, the hole injection current into the active region drops to 73 A/cm^2. The calculated turn-on bias is slightly higher than measured. However, the small differences between both cases are not sufficient to eliminate one of the droop explanations. Intermediate EBL acceptor densities would lead to a coexistence of both droop mechanisms in this simulation.

Additional characteristics are needed to identify the dominating droop mechanism. An obvious next step is the variation of the stage temperature. Various groups measured a decline of the LED efficiency with an increasing ambient temperature.[25–27] We here investigate this effect by increasing the temperature in both simulations to T = 150 °C, without changing any other parameter. The resulting internal quantum efficiency (IQE) is plotted in Fig. 3. At room temperature, electron leakage gives a somewhat higher IQE than Auger recombination. Unfortunately, this difference does not help to clearly separate both droop mechanisms from each other because the measured external quantum efficiency

This article is copyrighted as indicated in the article. Reuse of AIP content is subject to the terms at: http://scitation.aip.org/termsconditions. Downloaded to IP: 173.75.255.93 On: Mon, 20 Jul 2015 13:56:11

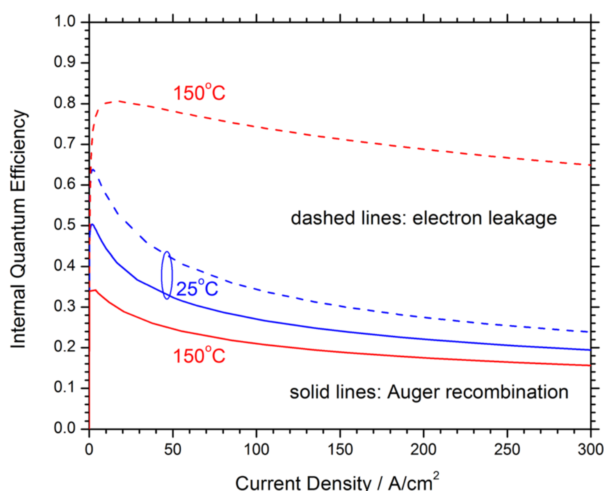

FIG. 3. Internal quantum efficiency vs. current density calculated at different ambient temperatures (solid lines—simulation favouring Auger recombination and dashed lines—simulation favouring electron leakage).

(EQE) depends on the photon extraction efficiency (EXE) which is not exactly known (EQE = IQE × EXE). But EXE is usually assumed constant so that the normalized IQE curve is the same as the normalized EQE curve, as in Fig. 1. However, rising ambient temperature leads to strikingly different efficiency changes in Fig. 3, which will be investigated in the following paragraphs.

Contrary to common assumptions, the dashed lines in Fig. 3 indicate that electron leakage from the QWs is reduced at higher temperature. This is attributed to an enhanced hole transport.[9] The large Mg acceptor ionization energy leads to a very small hole density at room temperature. Increasing temperature improves acceptor ionization and produces more free holes in the p-doped layers, as shown in Fig. 4. This leads to stronger hole injection into the active region and more uniform hole distribution among the five quantum wells (Fig. 4). At 300 A/cm^2 total current density, the calculated hole injection current into the MQW rises from 73 A/cm^2 at room temperature to 200 A/cm^2 at 150 °C. The electron leakage from the MQW is reduced correspondingly

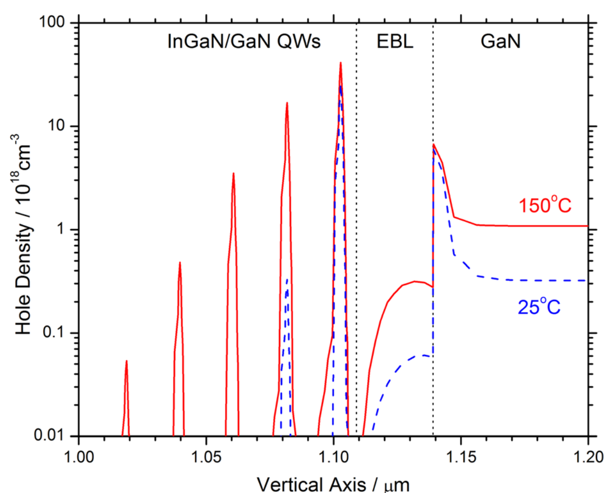

FIG. 4. Vertical hole density profiles calculated at 300 A/cm^2 injection current density for different ambient temperatures T in the case of dominating electron leakage (solid line—T = 150 °C and dashed line—T = 25 °C).

and the quantum efficiency rises. However, this simulated temperature sensitivity is opposite to experimental observations. In other words, electron leakage based on thermionic emission is unable to explain the measured efficiency reduction with higher temperature. Electron leakage by tunnelling via defect levels is not included in this simulation because it is only relevant at very low current.[28] Leakage of high-energy (hot) electrons generated by Auger recombination is negligible in this case with $C = 10^{-34}$ cm^6/s. In the other words, electron leakage can be eliminated as primary cause of the room-temperature efficiency droop in these LEDs. Any high-current electron leakage is rooted in the low hole conductivity of p-doped layers,[29] and is therefore expected to exhibit a similar temperature sensitivity. Our conclusion is confirmed by recent emission spectrum measurements on blue LEDs.[26] These measurements directly detect electron leakage by observing additional emission at shorter wavelength near 400 nm, but only at very low temperatures ($T < -100$ °C) and not near room temperature.

On the other hand, using the parameter set favouring Auger recombination, the simulated efficiency drop with higher temperature confirms the general trend observed experimentally (solid lines in Fig. 3). The Auger coefficient is considered temperature independent in this study, since published reports on C(T) are still inconclusive.[27] The simulated drop in peak efficiency by 30% is somewhat larger than the about 20% reduction measured on blue LEDs in the same temperature range.[3,25,27] The difference suggests a decline of the Auger parameter with rising temperature[27] or *minor* contributions from thermionic emission leakage in these experiments. Leakage of hot Auger electrons into the p-doped layers is not considered here because the travel distance of hot electrons remains unclear. While some experiments show hot electron emission from the p-side surface of GaN-based LEDs,[30] others measure hot electron capture by neighbouring QWs.[31] Monte-Carlo models support a rather short travel distance,[32] even for bulk GaN.[33] Other models assume a certain travel distance without consideration of hot electron scattering mechanisms.[34,35] However, such *secondary* leakage of hot Auger electrons would simply lead to a smaller C-parameter in fitting efficiency measurements,[34] and would not change the conclusion of this study. The main reason for the efficiency reduction in our simulation at 300 A/cm^2 is the decline in radiative recombination current from 57 A/cm^2 at room temperature to 45 A/cm^2 at 150 °C. Such reduction of the QW emission rate was also suggested by other investigations of temperature effects.[25,27,36] Our calculated emission spectra are plotted in Fig. 5. The thermal red-shift of the emission peak translates into a QW bandgap shift of 0.6 meV/K and is in agreement with measurements.[37]

In conclusion, advanced numerical simulations of the GaN-LED efficiency variation with rising temperature lead to a clear distinction between electron leakage and Auger recombination as dominating cause of the efficiency droop. The electron leakage model predicts an increasing efficiency with higher temperature, but published measurements on blue LEDs established an opposite trend. Thus, while electron leakage may still have a minor influence, it can be excluded as primary cause of the efficiency droop in these LEDs. On the other hand, the Auger recombination model

This article is copyrighted as indicated in the article. Reuse of AIP content is subject to the terms at: http://scitation.aip.org/termsconditions. Downloaded to IP: 173.75.255.93 On: Mon, 20 Jul 2015 13:56:11

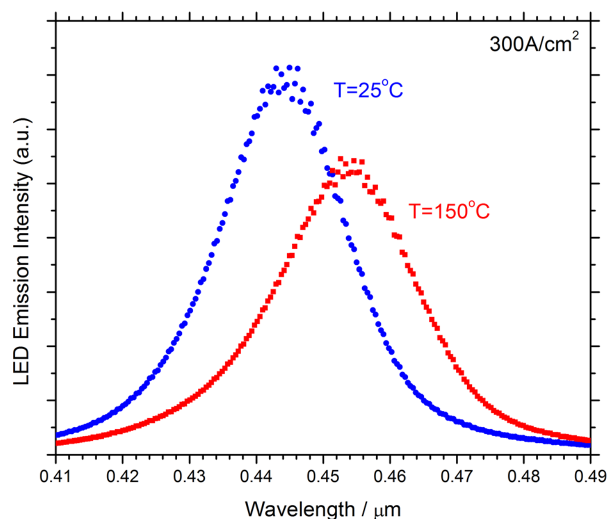

FIG. 5. Total emission spectrum from all quantum wells as calculated at different ambient temperatures in the case of dominating Auger recombination.

reproduces the measured efficiency behaviour almost perfectly. However, the surprisingly strong Auger recombination in InGaN quantum wells is still not fully understood and further investigations are needed to clarify its influence. Recent simulations of compositional quantum-well fluctuations indicate Auger recombination enhancements by local carrier accumulation.[38]

[1] J. Piprek, Phys. Status Solidi A **207**, 2217–2225 (2010).
[2] G. Verzellesi, D. Saguatti, M. Meneghini, F. Bertazzi, M. Goano, G. Meneghesso, and E. Zanoni, J. Appl. Phys. **114**, 071101 (2013).
[3] M. H. Kim, M. F. Schubert, Q. Dai, J. K. Kim, E. F. Schubert, J. Piprek, and Y. Park, Appl. Phys. Lett. **91**, 183507 (2007).
[4] Y. C. Shen, G. O. Mueller, S. Watanabe, N. F. Gardner, A. Munkholm, and M. R. Krames, Appl. Phys. Lett. **91**, 141101 (2007).
[5] J. Hader, J. V. Moloney, and S. W. Koch, Proc. SPIE **9003**, 900311 (2014).
[6] APSYS by Crosslight Software, Inc., Vancouver, Canada, 2014.
[7] V. Fiorentini, F. Bernardini, and O. Ambacher, Appl. Phys. Lett. **80**, 1204 (2002).
[8] J. Piprek and S. Li, *Optoelectronic Devices: Advanced Simulation and Analysis*, edited by J. Piprek (Springer, New York, 2005), Chap. 10.
[9] J. Piprek and S. Li, Opt. Quantum Electron. **42**, 89–95 (2010).
[10] M. E. Zvanut, U. R. Sunay, J. Dashdorj, W. R. Willoughby, and A. A. Allerman, Proc. SPIE **8262**, 82620L (2012).
[11] J. Piprek and S. Li, Appl. Phys. Lett. **102**, 131103 (2013).
[12] F. Römer and B. Witzigmann, J. Comput. Electron. **14**, 456 (2015).
[13] J. Piprek, F. Römer, and B. Witzigmann, Appl. Phys. Lett. **106**, 101101 (2015).
[14] K. T. Delaney, P. Rinke, and C. G. Van de Walle, Appl. Phys. Lett. **94**, 191109 (2009).
[15] F. Bertazzi, M. Goano, and E. Bellotti, Appl. Phys. Lett. **97**, 231118 (2010).
[16] G. Hatakoshi and S. Nunoue, Jpn. J. Appl. Phys., Part 1 **52**, 08JG17 (2013).
[17] E. Kioupakis, Q. Yan, and C. G. Van de Walle, Appl. Phys. Lett. **101**, 231107 (2012).
[18] F. Bertazzi, M. Goano, and E. Bellotti, Appl. Phys. Lett. **101**, 011111 (2012).
[19] J. Hader, J. V. Moloney, and S. W. Koch, Appl. Phys Lett. **92**, 261103 (2008).
[20] F. Bertazzi, X. Zhou, M. Goano, G. Ghione, and E. Bellotti, Appl. Phys. Lett. **103**, 081106 (2013).
[21] F. Bertazzi, X. Zhou, M. Goano, G. Ghione, and E. Bellotti, in Proceedings of 14th International Conference on Numerical Simulation of Optoelectronic Devices (2014).
[22] R. Vaxenburg, A. Rodina, E. Lifshitz, and A. L. Efros, Appl. Phys. Lett. **103**, 221111 (2013).
[23] R. Vaxenburg, E. Lifshitz, and A. L. Efros, Appl. Phys. Lett. **102**, 031120 (2013).
[24] M. Schubert, J. Xu, J. K. Kim, E. F. Schubert, M. H. Kim, S. Yoon, S. M. Lee, C. Sone, T. Sakong, and Y. Park, Appl. Phys. Lett. **93**, 041102 (2008).
[25] D. S. Meyaard, Q. Shan, Q. Dai, J. Cho, E. F. Schubert, M. H. Kim, and C. Sone, Appl. Phys. Lett. **99**, 041112 (2011).
[26] D. S. Shin, D.-P. Han, J.-Y. Oh, and J.-I. Shim, Appl. Phys. Lett. **100**, 153506 (2012).
[27] I. E. Titkov, S. Y. Karpov, A. Yadav, V. L. Zerova, M. Zulonas, B. Galler, M. Strassburg, I. Pietzonka, H.-J. Lugauer, and E. U. Rafailov, J. Quantum Electron. **50**, 911 (2014).
[28] M. Auf der Maur, B. Galler, I. Pietzonka, M. Strassburg, H. Lugauer, and A. Di Carlo, Appl. Phys. Lett. **105**, 133504 (2014).
[29] D. S. Meyaard, G.-B. Lin, Q. Shan, J. Cho, E. F. Schubert, H. Shim, M.-H. Kim, and C. Sone, Appl. Phys. Lett. **99**, 251115 (2011).
[30] J. Iveland, L. Martinelli, J. Peretti, J. S. Speck, and C. Weisbuch, Phys. Rev. Lett. **110**, 177406 (2013).
[31] M. Binder, A. Nirschl, R. Zeisel, T. Hager, H.-J. Lugauer, M. Sabathil, D. Bougeard, J. Wagner, and B. Galler, Appl. Phys. Lett. **103**, 071108 (2013).
[32] T. Sadi, P. Kivisaari, J. Oksanen, and J. Tulkki, Appl. Phys. Lett. **105**, 091106 (2014).
[33] F. Bertazzi, M. Goano, X. Zhou, M. Calciati, G. Ghione, M. Matsubara, and E. Bellotti, Appl. Phys. Lett. **106**, 061112 (2015).
[34] F. Römer, M. Deppner, C. Range, and B. Witzigmann, Proc. SPIE **8986**, 89861R (2014).
[35] Z. M. S. Li, J. Comput. Electron. **14**, 409 (2015).
[36] J. Hader, J. V. Moloney, and S. W. Koch, Appl. Phys. Lett. **99**, 181127 (2011).
[37] S. Nakamura, S. Pearton, and G. Fasol, *The Blue Laser Diode*, 2nd ed. (Springer, Berlin, 2000), p. 299.
[38] C.-K. Wu, C.-K. Li, and Y.-R. Wu, J. Comput. Electron. **14**, 416 (2015).

This article is copyrighted as indicated in the article. Reuse of AIP content is subject to the terms at: http://scitation.aip.org/termsconditions. Downloaded to IP: 173.75.255.93 On: Mon, 20 Jul 2015 13:56:11